Neurotoxicology 73 (2019) 246–257

Contents lists available at ScienceDirect

Neurotoxicology

journal homepage: www.elsevier.com/locate/neuro

Full Length Article

Prolong treatment with Trans-ferulic acid mitigates bioenergetics loss and restores mitochondrial dynamics in streptozotocin-induced sporadic dementia of Alzheimer's type

Mohd Faraz Zafeer[a,*], Fakiha Firdaus[a,b], Ehraz Anis[a], M Mobarak Hossain[a]

[a] Interdisciplinary Brain Research Centre, Faculty of Medicine, Aligarh Muslim University, Aligarh, India
[b] Department of Zoology, Faculty of Life Sciences, Aligarh Muslim University, Aligarh, India

ARTICLE INFO

Keywords:
Alzheimer's disease
Mitochondrial dynamics
PGC-1aplha
OXPHOS
mPTP Opening
Intracerebroventricular streptozocin injections

ABSTRACT

Alzheimer disease has been well associated with mitochondrial dysfunctions. Numerous studies have reported changes in the activity of oxidative phosphorylation (OXPHOS) complexes and mitochondrial dynamics. Recently, dynamin-related protein 1 (Drp-1) has been conceived as a potential therapeutic target as well. We have examined the effect of prolonged treatment of Trans-ferulic acid on streptozocin-induced sporadic dementia of Alzheimer's type. We have found the Ferulic Acid (FA,100 mg/kg) can rescue memory and learning problems and also show significant antioxidant effect while preserving morphology of pyramidal cell layer in hippocampi.

Furthermore, FA treatment has shown mitigation in intracerebral-ventricular streptozocin (ICV-STZ) induced bioenergetics loss and dynamic changes by regulating peroxisome proliferator-activated receptor gamma coactivator 1-alpha (PGC-1alpha) protein levels in nucleus and hence, mitigating exacerbation of Drp-1 dependent mitochondrial fission and apoptosis by alleviating loss of mitochondrial membrane potential ($\Delta\Psi m$), downregulating cytochrome-c release into the cytosol by limiting mitochondrial permeability transition pore (mPTP) opening concomitant increase in caspase3 activation, BAX expression and DNA fragmentation along with downregulating glial fibrillary acidic protein (GFAP) expression. FA also restored protein expression of mitofusin2 (Mfn2) a core component of mitochondrial fusion, necessary for mitophagy. We conclude that FA acid may have the propensity to mitigate mitochondrial dysfunction in Alzheimer's disease on prolonging dietary supplementation.

1. Introduction

Alzheimer's disease (AD) is a progressive neurodegenerative disorder associated with age (Selkoe and Lansbury, 1999). With the progress in degenerative changes patients of AD show lack of reminiscence and cognitive deficiencies (Choi and Twamley, 2013). It disturbs everyday life because of the decline of cognitive skills, compromises behavioral competence and linguistics (Gutiérrez-Rexach and Schatz, 2016). In advance stages, patients cannot even recognize family members, which creates a nuisance in term of patient care (Robert et al., 2010). The signs and symptoms of AD vary from person to person and are generally ignored in the first few years of its inception. Forgetfulness is the typical primary signal for the beginning of AD (Jahn, 2013). Subsequently, the affected person develops full AD pathology with severe cognitive impairment, wherein patients are not able to communicate and are ignorant of the surrounding, with profound bodily dependence on caregivers for each day chores (Kelley and Petersen, 2007). AD has been recognized as the "worldwide public health priority" by the World Health Organization (WHO, 2012). Epidemiological research in 2015 has proven that AD and associated dementia impacts forty-seven million people worldwide (Cornutiu, 2015; Russ et al., 2015). Currently, 36 million people older than sixty-five years are living with dementia and these figures are expected to swell to 66 million and 115 million by 2030 and 2050 respectively [UN (DESA), 2015]. With the increment in the average human lifespan, AD has all the likelihood to emerge as an exceptional healthcare challenge.

Impaired mitochondrial dynamics have been extensively implicated in AD (Gao et al., 2017). Dynamics generally refer to the process by which mitochondria population is regulated. It consists of two processes namely fusion and fission. Primarily the process of dynamics is highly dependent upon the localization of conserved proteins, the dynamin-associated GTPases on the mitochondrial surface (Mishra and Chan,

* Coressponding author at: Interdisciplinary Brain Research Centre, Faculty of Medicine, Aligarh Muslim University, Aligarh, Uttar Pradesh, India.
E-mail address: faraz.zafeer@gmail.com (M.F. Zafeer).

https://doi.org/10.1016/j.neuro.2019.04.006
Received 8 September 2018; Received in revised form 12 April 2019; Accepted 12 April 2019
Available online 25 April 2019
0161-813X/

2016). Mitochondrial fission is essential for mitochondrial renewal, redistribution, and proliferation inside synapses; while mitochondrial fusion facilitates mitochondrial movement and distribution throughout axons and to the synapses themselves (Cheng et al., 2010). A balance between those two events is vital to maintaining purposeful mitochondrial integrity (Safiulina and Kaasik, 2013). Analysis of transgenic and non-transgenic animal models of AD along with human post-mortem samples have confirmed downfall of the Mnf1, Mnf2, and Opa1 fusion genes and increased expression of fission genes Drp-1 and Fis1 (Zhu et al., 2013; Manczak et al., 2011; Wang et al., 2009).

Oxidative stress is believed to be an early manifestation of AD (Gella and Durany, 2009). Studies of post-mortem AD brains indicate widespread oxidative damage, Brains from individuals affected with AD further display increased protein oxidation, as evidenced by carbonyl-alterations of specific proteins (Ganguly et al., 2017; Gomez-Nicola and Boche, 2015; Ansari and Scheff, 2010). Accumulating data suggest mitochondrial function, if not changes in cell bioenergetics or the pathways that regulate cell bioenergetics, are perturbed early in the course of AD (Swerdlow, 2012). If so, then therapies directed towards mitochondrial abnormalities may benefit affected patients to some degree. It may also be the case that mitochondrial or bioenergetics dysfunction may constitute in the early etiology of AD (Wallace, 2013).

Trans-Ferulic acid (FA,4-hydroxy-3-methoxy cinnamic acid) is found in many grains such as wheat, rice bran, and maize bran (Mathew and Abraham, 2004). Intriguingly, FA has also been found in some vegetables such as artichokes and aubergines (Kumar and Pruthi, 2014). Additionally, FA has been reported to have antioxidant, anti-inflammatory and mito-protective efficacies (Wu et al., 2014; Zhu et al., 2014; Lin et al., 1994). Ferulic acid has been found to have a mitigatory role in diabetic neuropathy. Moreover, Picone et al. (2013) showed that FA could alleviate Aβ induced ROS expedited oxidative stress in sea urchin embryo. Furthermore, Yan et al. (2001) have reported the protective effects of long-term administration of FA against β amyloid-induced astrogliosis and memory impairment. However, there are is no report about the effects of FA on sporadic dementia and related mitochondrial perturbations. Besides, current researches about the antioxidant mechanisms of FA mostly focus on scavenging of free radicals and its impact on mitochondrial dysfunctions has not been reported. So, in the current study, we have examined the effect of FA on the ICV-STZ induced oxidative damage, apoptosis and mitochondrial perturbation such as bioenergetics loss and dynamics changes.

2. Material and methods

2.1. Chemicals

Streptozocin (STZ), Trans-ferulic acid, Anti-Mfn2 antibody, DCFDA, TMRE, Propidium iodide, and DAPI were procured from Sigma-Aldrich (MO, USA). Drp-1 primary antibody was purchased from Abcam (Cambridge, UK). Anti-BAX, Anti Cytochrome-C, Anti-mouse secondary, and anti-rabbit secondary antibodies were procured from Santa Cruz Biotechnology (USA). OXPHOS cocktail, Hibernate A, B27, and Anti-PGC1-alpha antibody was purchased from Thermo Scientific (USA). The anti-GFAP antibody was procured from cell signaling technology (USA). All other general chemicals were acquired for Merck India Pvt Ltd.

2.2. Animals

Male Wistar rats (350 ± 25gm) were procured from the central animal house facility, Jawaharlal Nehru Medical College and maintained at 25 ± 20 °C in a well-ventilated room with ad-libitum feed and water. The institutional ethics committee approved all the animal experimentation protocols as per the CPSEA guidelines, Govt. of India.

2.3. Intracerebroventricular injection of STZ

Rats were anesthetized with 75 mg/kg Ketamine (i.p) and 5 mg/kg Diazepam (i.p). The depth of anesthesia was measured with a toe pinch, and their skull was shaved. Post-anaesthesia animals were mounted on the stereotaxic frame (Steolting, IL, USA) and ear bars were gently inserted, the body temperature of the animal was maintained using a heating pad to avoid anesthesia-related hypothermia. The skull was cleaned twice with 70% ethanol, and 10% povidone-iodine solution and a fine midline incision of 2–3 cm was done to expose the bregma. Burr holes for ICV-STZ injections were made as per the coordinates provided in Paxinos and Watson (1986), i.e. (−1.5 mm lateral, −0.8 mm posterior and −3.6 mm below). STZ was injected at a dose of 3 mg/kg, 5 µl per ventricle using a 28 gauge Hamilton syringe at a rate of 0.5 µl per minute. post-injection the needle was left in place for additional 5 min to ensure the proper diffusion of STZ. after the injections the burr holes were sealed using commercially available sterile bone wax and the incision was closed using 4-0 Ethicon prolene sutures. Animals were given a bolus of 1 ml dextrose normal saline (i.p) and were given a single dose 2 mg/kg meloxicam (i.p) and 10,000 unit of penicillin (i.m), for management of pain and prevention against infections immediately after surgery.

2.3.1. Post-operative care

Animals were maintained at 37 °C until they gained complete motor control, they were housed individually for the first two days and were provided with moistened feed pellets and water inside the cage, to avoid neck trauma.

2.4. Groups

1.	Sham:	Rats received ICV injection of vehicle (normal saline) along with Oral gavages of Corn oil.
2.	Lesion:	Rats received ICV-STZ 3 mg/kg only.
3.	Lesion + FA:	Rats received ICV-STZ 3 mg/kg along with FA (100 mg/kg; p.o.) in Corn oil.
4.	Sham + FA:	Rats received ICV injection of vehicle (normal saline) along with FA (100 mg/kg; p.o.).

2.5. Assessment of cognitive impairment by Morris Water Maze

Spatial learning and memory of animals were tested in Morris water maze, consisting of a circular water tank (132 cm diameter and 60 cm height) filled with 30 cm water (25 ± 2 °C). The non-toxic black paint was used to make water opaque. The pool was virtually divided into four quadrants, namely NE, NW, SE, and SW. A platform (10 cm in

diameter) was hidden 2 cm below the surface of the water on a fixed location in one of the four quadrants of the pool. Before training started, rats were allowed to swim freely into the pool for 60 s without a platform. They were then given four trials (once from each starting position) per session for five days, each test having a ceiling time of 60 s and a trial interval of approximately 30 s. After climbing onto the platform, the animal remained there for 30 s before the commencement of the next trial. If a rat could not perform the task of finding the hidden platform, it was placed manually on the platform and allowed to stay there for a time of additional 60 s.

An overhead video camera was connected to a video monitor, and Any Maze Video Tracking Software (Steolting, IL, U.S.A) was used to track the animal's path and escape latency.

2.6. Hippocampal isolation

Animals were anesthetized using 75 mg/kg of ketamine and sacrificed using cell dislocation. Brains were immediately isolated in ice-cold phosphate buffer (0.1 M, pH 7.4). Hippocampi were isolated manually using dissection spatula and immediately frozen for western blot analysis and kept in hibernate media supplemented with B27 for flow cytometry and comet assay sample preparation.

2.7. Preparation of single cell suspension for flow cytometry

Hippocampi were isolated and kept in 2 ml hibernate media supplemented with B27. Individual hippocampi were treated with 0.25% trypsin-EDTA for 2 min at 37 °C. Post incubation hippocampi were gently triturated using a fire-polished glass pipette, and the single cell suspension was passed through a sterile mesh of 70 microns. The cell suspension was then centrifuged at 125 g for 5 min, and the pellet was suspended in fresh hibernate media containing B27.

2.8. Analysis of intracellular ROS generation by DCFDA

Intracellular ROS generation was analyzed by using 2′,7′-dichlorofluorescein diacetate (DCFDA), which is a selective fluorescent probe for ROS. DCFDA after diffusion into the cell undergoes deacetylation to a non-fluorescent compound, which is later oxidized by ROS into 2′,7′-dichlorofluorescein (DCF) which is a highly fluorescent compound. Single cell suspension in hibernate media supplemented with B27 was incubated in 10 μM DCFDA for 30 min at 37 °C in the dark. Following the incubation cells were again pelleted at 125 g for 5 min and suspended in new hibernate A medium with B27 supplement. Flow cytometric acquisitions of 10,000 events were made using BD-LSR II flow cytometer at £x/£m: 495 nm/529 nm. Histograms were generated using FACS-DIVA analysis software.

2.9. Measurement of mitochondrial membrane potential ($\Delta\psi m$)

Mitochondrial Membrane Potential ($\Delta\psi m$) was analyzed by flow cytometric analysis using TMRE (tetra-methyl rhodamine, ethyl ester). TMRE is a red-orange, cell-permeant, a positively charged dye that is readily accumulated into the mitochondria, due to their overall negative charge. Depolarised of compromised mitochondria will have lower membrane potential and hence lesser ability to collect TMRE. Single cell suspensions in hibernate A media supplemented with B27 were incubated with 10μM TMRE for 30 min at 37 °C in the dark, post-incubation cells were pelleted by centrifugation at 125 *g* for 5 min. and suspended in the B27 supplemented hibernate A medium. The flow cytometric acquisition of fluorescent intensities from 10,000 events was made using BD-LSR II cell analyzer at £x/£m: 549/574 and histograms were generated using FACS-DIVA analysis software.

2.10. Assessment of mitochondrial lipid peroxidation (LPO)

Analysis of mitochondrial damage due to Oxidative stress concomitant membrane damage was performed by using the method of Uchiyama and Mihara (1978). The results were expressed as nmoles of TBARS formed/ h/mg protein of isolated mitochondria using a molar extinction coefficient (MEC) $1.56 \times 10^5\ M^{-1}\ cm^{-1}$.

2.11. Assessment of F_1–$F_O$synthase activity for analysis of ATP synthesis

ATP synthase is also referred to as mitochondrial complex V. Its activity was assayed as, hydrolysis of ATP into ADP plus inorganic phosphate (Pi). The absorbance was measured at 660 nm. The enzyme activity was expressed as microgram of Pi liberated per minute per milligram protein (Waseem and Parvez, 2015).

2.12. Assessment of DNA fragmentation by comet assay

Cell suspensions were mixed with 0.5% (w/v) low melting agarose and overlaid on slides precoated with 1% (w/v) standard melting agarose and coated with a third layer of 1% (w/v) low melting agarose. Slides were then immersed overnight in a lysing solution briefly containing NaCl (2.5 M), EDTA (100 mM), Trizma base (10 mM), NaOH (0.2 mM), 1% Triton X-100 and DMSO (pH 10) at 4 °C. on the subsequent day cells were incubated with an alkali unwinding solution containing (300 mM NaOH, 1 mM EDTA, pH > 13) for 20 min. Slides were then immersed in cold TBE for 10 min and subjected to Electrophoresis at 25 V in 1X TBE buffer for 45 min. Slides were stained with propidium iodide (1X) solution and dried overnight. Photographs were obtained at 40X magnification using Nikon Eclipse Ci-L fluorescence microscope. Comets for analysis were selected randomly and analyzed with Comet score software 2.0 (TriTek corporation, USA).

2.13. Assessment of mPTP opening by Calcein-AM/CoCl2 assay

mPTP opening in cells of hippocampi of rats was evaluated using Calcein-AM/ $CoCl_2$ assay method. The evaluation was grounded on the capability of $CoCl_2$ to quench Calcein fluorescence in the cytosol, and the mitochondria with open mitochondrial permeability transition pore, the mitochondria with intact mPTP activity will preserve Calcein fluorescence as $CoCl_2$ will be incapable of entering them. Briefly, cells are incubated with 5μM Calcein-AM for 30 min at 37 °C, following termination of incubation cell suspension was washed and incubated with 40 μM $CoCl_2$ for 20 min at 37 °C. Cells were washes by centrifuged at 125 g for 5 min. and resuspended in fresh hibernate medium supplemented with B27. The flow cytometric acquisition of fluorescent intensities from 10,000 events was made using BD-LSR II cell analyzer and histograms were generated using FACS-DIVA analysis software.

2.14. Preparation of subcellular fractions and western blotting

Hippocampi were homogenized using a Dounce homogenizer in isotonic HEPES isolation media (20 mM HEPES pH 7.4, 0.25 M sucrose, 10 mM KCl, 1.5 mM MgCl2, 1 mM EGTA, 1 mM EDTA) supplemented with protease inhibitors (1 mg/ml pepstatin, 10 mg/ml aprotinin, 10 mg/ml leupeptin), and then centrifuged at 750 x g for 10 min. The resulting pellet was taken as the nuclear fraction, and the supernatant was centrifuged at 14,000 x g for 10 min, and the pellet was re-suspended in 0.25 M sucrose, 0.5 Mm EDTA adjusted by Tris to pH 7.4 and was used as a crude mitochondrial fraction. The remaining supernatant was centrifuged at 100,000 x g for 60 min, and the supernatant was taken as the cytosolic fraction. Protein estimation of the samples was done using the method of Bradford, 1976. SDS gels were cast using 10% TGX-Fast Cast Kit (Bio-Rad, CA, USA), and 35 μg of protein from each sample was transferred to a PVDF membrane (0.22 μm, Bio-Rad, Hercules, CA, USA) using a wet transfer unit (Bio-Rad, Hercules, CA,

USA). Post-transfer membranes were blocked for non-specific binding with 5% milk for 1 h and washed with PBST (0.05% Tween20). PVDF membranes were then incubated overnight with primary Drp-1, Mfn2, Cytochrome-c, BAX, Beta-Actin, PGC1-alpha, OXPHOS antibody cocktail at 4 °C with gentle shaking respectively. Subsequently, the membrane was washed thrice by PBST and incubated with HRP-conjugated secondary antibodies (1:2000) dilution Santa Cruz Biotechnology, CA, USA) at room temperature for 1.5 h. Finally, the membrane was treated with super signal ECL substrate (Pierce, Thermo, USA) for 3–5 minutes, and the signals were visualized using a Chemi-Doc system at different exposure times (Bio-Rad, CA, USA).

2.15. Hematoxylin and eosin staining

The animals were anesthetized with 75 mg/kg ketamine and 5 mg/ml diazepam intraperitoneally and perfused transcardially with ice-cold PBS (0.1 M, pH 7.4) followed by cold 4% Neutral buffered formalin in PBS (0.1 M pH 7.4). Brains were removed quickly, post-fixed in 4% Neutral buffered formalin solution for 48 h, dehydrated in graded alcohol and embedded in wax. Coronal sections having hippocampus and 5-micron thickness was dewaxed, and sections were stained using Hematoxylin followed by eosin solution for 5–8 min. The sections were then rinsed in distilled water and differentiated in alcohol followed by clearing in xylene and mounting in DPX. Images were acquired using a light microscope (Nikon ECIL, JPN) and area analysis of cells in the CA1 region was done using ImageJ (NIH, USA).

2.16. Immunohistochemistry (IHC) of GFAP

For IHC coronal sections were dewaxed and rehydrated in graded alcohol, antigen retrieval was done using citrate buffer (10 mM, pH 6.0). Followed by blocking using 1%BSA and incubation with 1:50 dilution of primary antibody overnight at 4 °C and 1:1000 FITC conjugated secondary antibody with proper washing. Slides were mounted in 60% glycerol and visualized in Nikon-ECIL fluorescence microscope.

2.17. Statistical analysis

Statistical analysis was done using GraphPad Prism 7 (GraphPad, CA, USA) using Analysis of Variance (ANOVA) and Tuckey's as a post-hoc test. A difference of ($p \leq 0.05$) was considered significant.

3. Results

3.1. FA alleviates ICV-STZ induced spatial learning and memory impairment

STZ induced significant learning impairment at 3 mg/kg dose, as evidenced by escape latency, i.e., the time taken to find the hidden platform (Fig. 1b), along with a considerable loss in memory recall as the STZ conditioned rat has spent less time the target quadrant of the water maze (Fig. 1c). FA significantly prevented the spatial memory and learning loss by as evidenced the increased ability of the FA treated rats to locate the target quadrant (##$p \leq 0.01$) and maintenance of escape latency(##$p \leq 0.01$).

3.2. Effect of ICV-STZ and FA on intracellular ROS generation

Analysis of the impact of ICV-STZ and FA on intracellular ROS generation was done by using DCFDA, which is a selective flow cytometric probe for ROS generation [Fig. 2], ICV-STZ exposure has been found to have exacerbated the levels of intracellular ROS in the hippocampi of rats when compared to the sham-operated rats (**$p \leq 0.01$). FA supplementation has been found to have a mitigatory effect on ICV-STZ induced ROS generation (#$p \leq 0.05$), suggesting its possible role in the mitigation of AD-related oxidative stress.

3.3. FA rescues (Δψm) in ICV-STZ treated rat hippocampi

loss of (Δψm) is considered as an early and obligate event on mitochondria-mediated apoptosis. (Δψm) was measured by flow cytometric analysis of TMRE, a particular probe (Fig. 3). Hippocampal cells in STZ exposed rats show significant depletion of (Δψm) (*$p \leq 0.05$). FA treatment has considerably protected (#$p \leq 0.05$) the levels of (Δψm) suggestive of its mito-protective efficacy.

3.4. FA mitigates ICV-STZ induced prolong mPTP opening

The effect of FA on ICV-STZ induced continue mPTP opening was analyzed by Calcein AM-cobalt quenching assay, based on quenching of intra-mitochondrial calcein fluorescence by cobalt influx through activated mPTP (Fig. 4). ICV-STZ conditioned rats brain hippocampi showed significant depletion (**$p \leq 0.01$) in mitochondrial Calcein-AM fluorescence following $CoCl_2$ exposure suggestive of prolonged

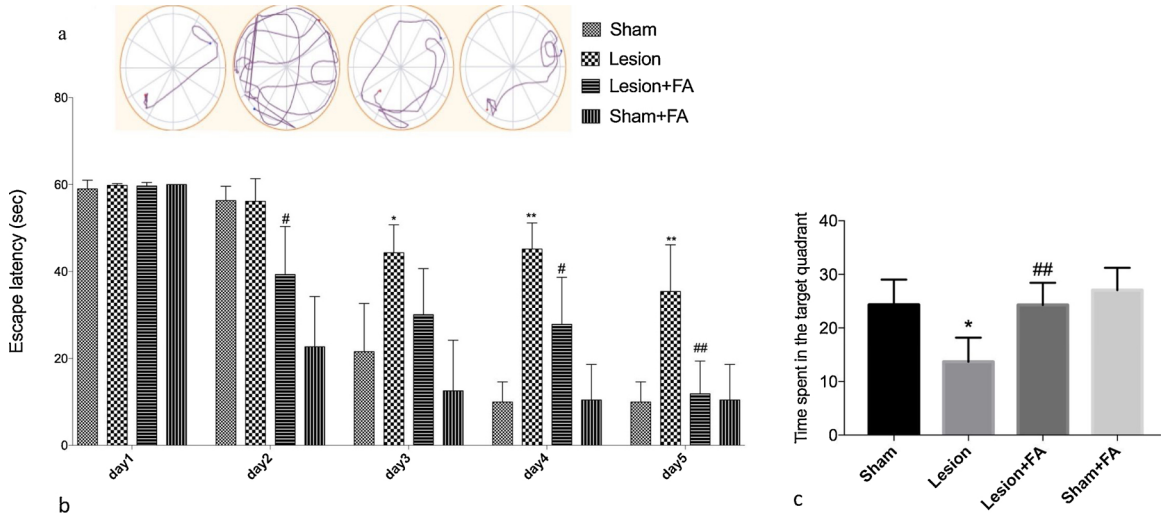

Fig. 1. Analysis of spatial memory and learning performance of rats (n = 6) in the Morris water maze, results are presented as Mean ± SEM. The significant difference is shown as (*$p \leq 0.05$) when compared to the sham group and as (#$p \leq 0.05$) when compared to the lesion group, fig1(a) Track plot images of escape latency generated by Anymaze Software (Steolting, USA), fig1(b) shows the escape latency of rats or the time taken by the rats to find the hidden platform during five days of trial, fig1(c) shows the time spent by the rats in the target quadrant in probe trial (when the hidden platform was removed).

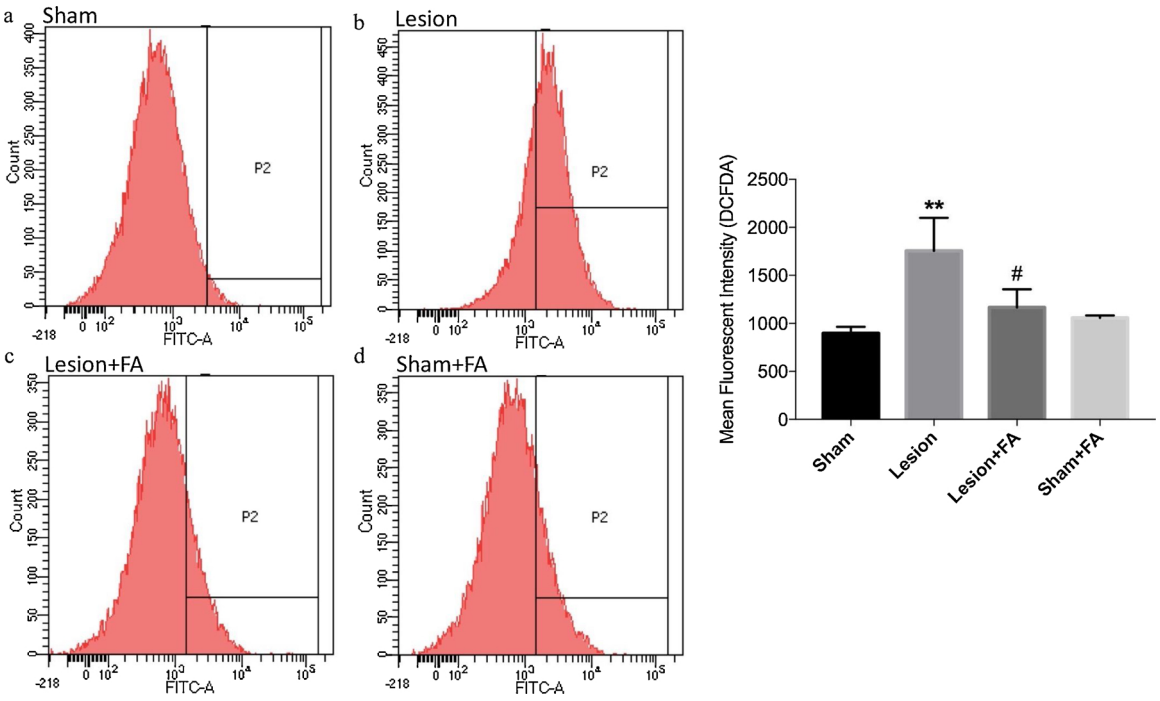

Fig. 2. Flow cytometric analysis of total ROS generation by DCFDA (n = 3). Cells were treated with 10 µM DCFDA for 30 min at 37 °C. Flow cytometric histograms a–d represent fluorescence intensities acquired in 10,000 events using £x/£m = 495/ 529 nm. Fig. 2 (a,b,c,d) represents Sham, Lesion, Lesion + FA, and Sham + FA conditioned rats respectively. The results are presented as Mean ± SEM. The significant differences are shown as (*p ≤ 0.05) when compared to the Sham group and as (#p ≤ 0.05) when compared to the Lesion group.

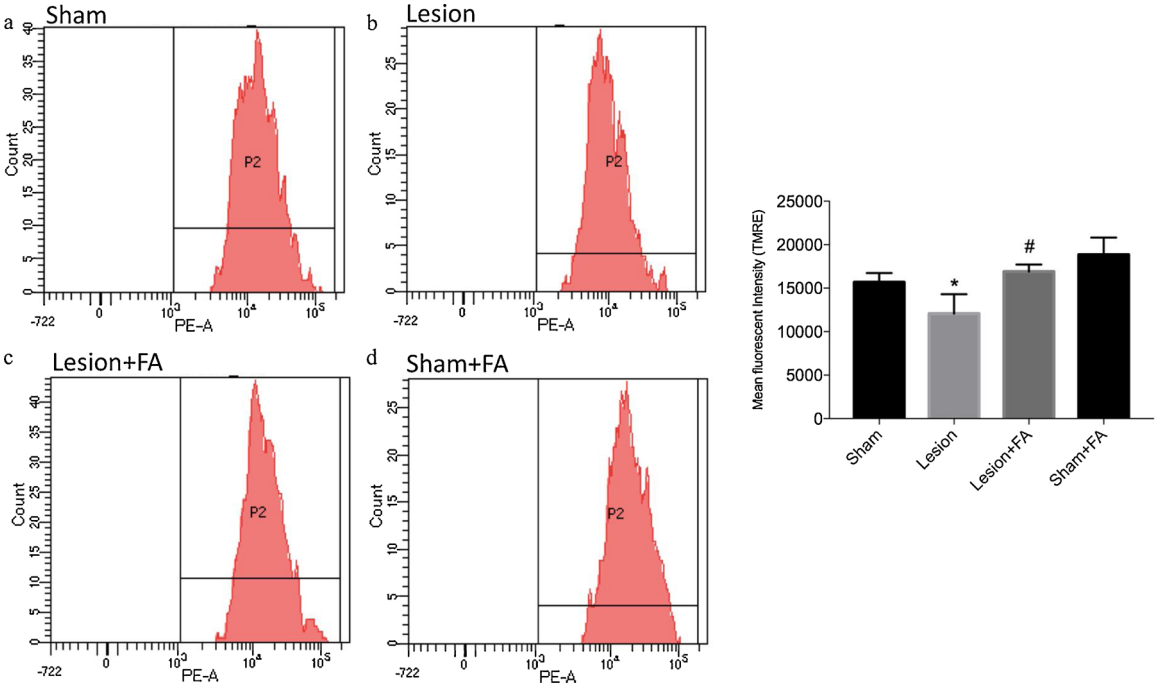

Fig. 3. Flow cytometric analysis of (Δψm) by TMRE (n = 3). Cells were treated with 10 µM Rh 123 for 30 min at 37 °C. Flow cytometric histograms a–d represent fluorescence intensities acquired in 10,000 events using £x/£m = 549/574 nm. Fig. 3 (a,b,c,d) represents Sham, Lesion, Lesion + FA, and Sham + FA conditioned rats respectively. The results are presented as Mean ± SEM. The significant differences are shown as (*p ≤ 0.05) when compared to the Sham group and as (#p ≤ 0.05) when compared to the Lesion group.

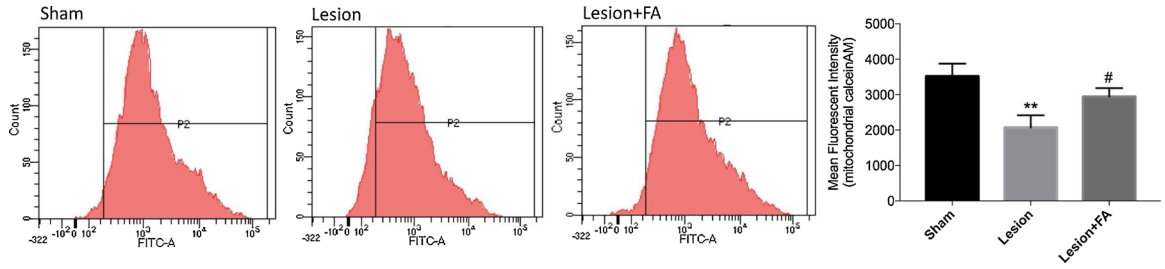

Fig. 4. Flow cytometric analysis of Effect of FA and ICV-STZ on mitochondrial permeability transition pore (mPTP) opening by Calcein-AM/$CoCl_2$ assay using flow cytometry (n = 3). Data was represented as Mean ± SEM. The significant difference is presented as (*p ≤ 0.05) when compared to the Sham group and as (#p ≤ 0.05) when compared to the Lesion group.

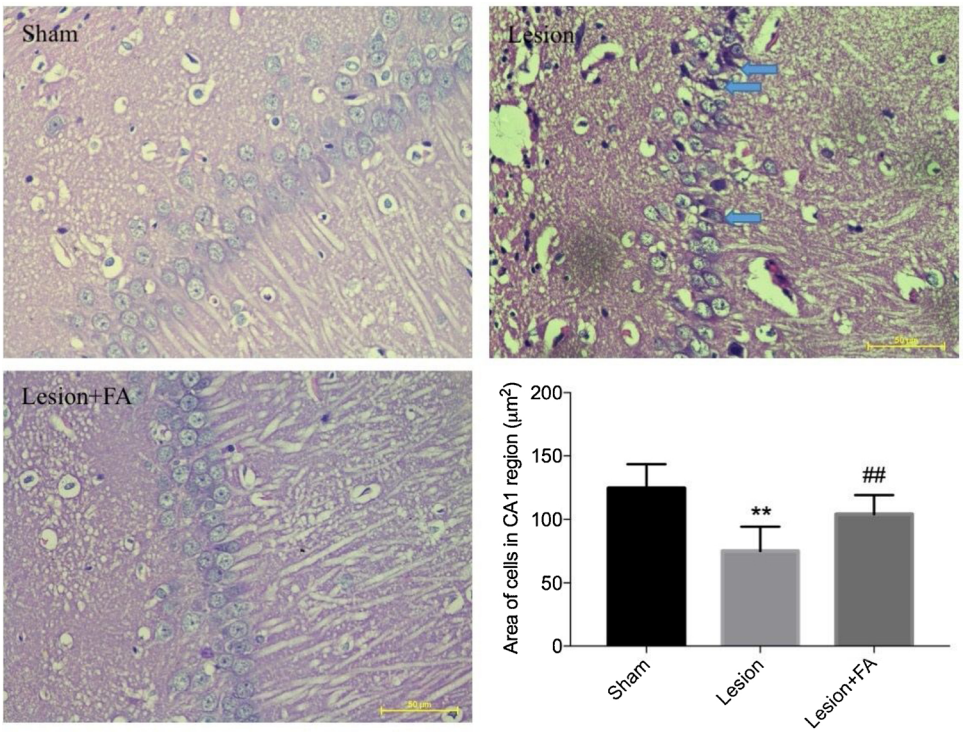

Fig. 5. Photomicrograph of H&E staining of coronal sections of the CA1 region of rat hippocampi from sham, lesion and lesion + FA groups respectively. The area analysis of 50 cells was done using ImageJ (NIH, USA) and results are expressed as Mean ± SEM. The significant difference is presented as (*p ≤ 0.05) when compared to the Sham group and as (#p ≤ 0.05) when compared to the Lesion group.

activation of mPTP due to worsening of mitochondrial ROS. FA treatment has significantly mitigated the prolong galvanization of mPTP (#p ≤ 0.05) in ICV-STZ conditioned rats.

3.5. Assessment of the effect of FA and ICV-STZ on pyramidal cell layer in the CA1 region

STZ administration through ICV causes significant changes (**p ≤ 0.01) in the area of the pyramidal cell layer along with extensive pyknosis suggestive of the neurodegenerative death of the hippocampal neurons (Fig. 5). Interestingly, FA treatment has restored the pyramidal cell layer morphology, as the cells appear rounder and more aligned, FA has also mitigated the cell shrinkage associated with the sporadic AD (##p ≤ 0.01).

3.6. Mitigatory role of FA on ICV-STZ induced DNA fragmentation

ICV-STZ causes a significant amount of DNA fragmentation as evidenced by an increase in comet tail length (Fig. 6d), comet area (Fig. 6e) and DNA in tail percentage (Fig. 6f; p ≤ 0.05) in the hippocampi of STZ conditioned rats. FA treatment was able to alleviate the DNA damage by reducing DNA content and length of comet tail (#p ≤ 0.05), suggestive of its ant apoptotic effect as STZ has been reported to have a robust alkylating impact of DNA and is known to cause DNA damage following exposure.

3.7. FA limits caspase 3 activation and astrogliosis

FA treatment has been found to have mitigated (##p ≤ 0.01; Fig. 8) levels of the caspase3 activation done by STZ (**p ≤ 0.01). Additionally, FA treatment has decreased the astrogliosis into the CA1 region of the ICV-STZ conditioned AD rats (Fig. 7). Ac-DEVD-pNA and GFAP provided a better picture of the apoptosis associated with ICV-STZ administration, as both are the early effectors of hippocampal apoptosis.

3.8. Effect of FA and ICV-STZ on mitochondrial localization of BAX and Cytochrome-C

The localization of BAX on mitochondria has been considered as an essential event in the process of apoptosis, BAX with BAK form large pores in the outer mitochondrial membrane which in turn causes mPTP opening and release of Cytochrome C into the cytosol. FA treatment has been found to have significantly (##p ≤ 0.01) alleviated ICV-STZ mediated internalization of BAX into the mitochondria (Fig. 11d) and Release of Cytochrome-C (#p ≤ 0.05) into the cytosol (Fig. 9d). These results collaborate with the findings of FA on Caspase 3 activation and mPTP opening (Fig. 4,8).

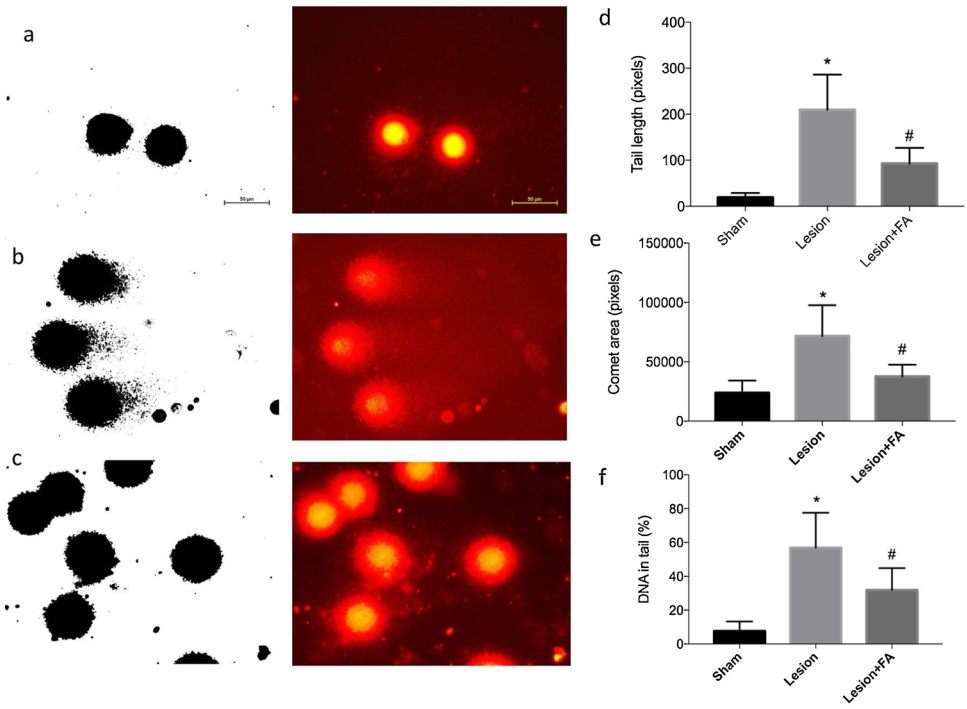

Fig. 6. Comet assay of the effect of FA on ICV-STZ induced DNA fragmentation. a,b,c represents images from Sham, Lesion, Lesion + FA groups respectively. (f) DNA percentage in tail, (e) comet area and (d) tail length were quantified using Cometscore (v2.0, Tritek, USA). Data was represented as Mean ± SEM. The significant difference is presented as (*p ≤ 0.05) when compared to the Sham group and as (#p ≤ 0.05) when compared to the Lesion group.

3.9. FA prevents ICV-STZ induced dysfunction in mitochondrial bioenergetics

ICV-STZ model of AD in accord with the human samples of AD has classically been reported to present changes in mitochondrial bioenergetics. STZ treatment has been found to have significantly down-regulated the OXPHOS complex I (NADH-CoQ oxidoreductase) Fig. 10b; *p ≤ 0.05, complex II (succinate dehydrogenase) Fig. 10c; *p ≤ 0.05 and complex IV (Cytochrome-c oxidase) Fig. 10e; (**p ≤ 0.01)] protein levels. Interestingly, FA treatment has been found to have a therapeutic effect (#p ≤ 0.05) on the OXPHOS protein complexes.

3.10. Role of FA in ICV-STZ related changes in mitochondrial dynamics

Drp-1 and Mfn2 have been considered as the master players in the

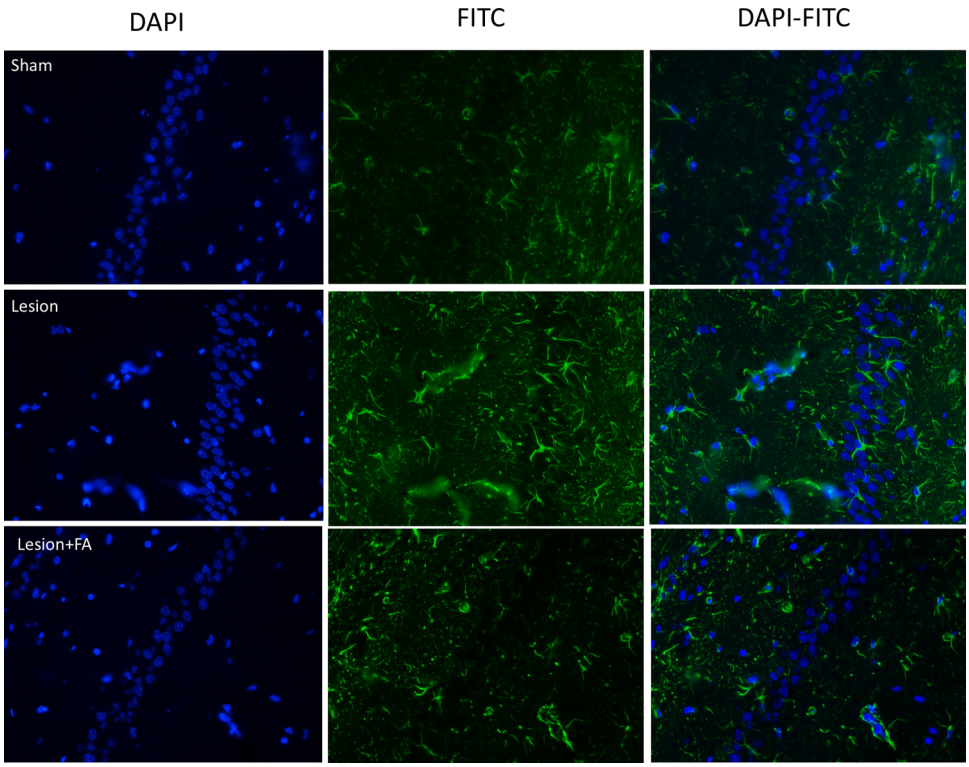

Fig. 7. Photomicrograph of the effect of FA and ICV-STZ on astrogliosis in hippocampi of rats. FITC conjugated secondary antibody was used, and the nucleus is counterstained with DAPI.

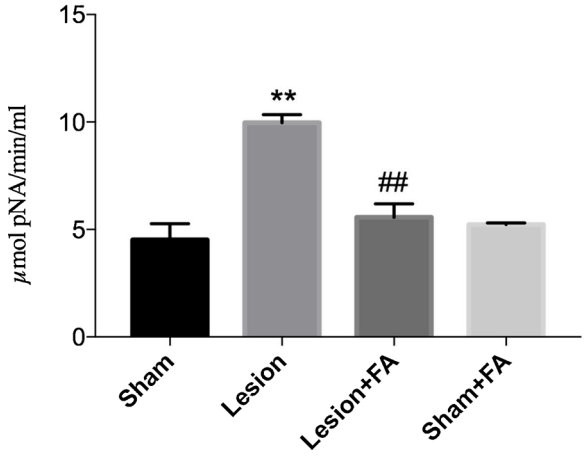

Fig. 8. Effect of FA on the ICV-STZ induced exacerbation in Caspase 3 activity using Ac-DEVD-pNA a selective probe for caspase3 having a maximum absorbance at 405 nm. Activity was measured regarding µM of pNA released/min/ml. Data was represented as Mean ± SEM. Significant differences are expressed as (*p ≤ 0.05) when the comparison was made with the Sham group and (#p ≤ 0.05) when compared with Lesion group.

delicate process of fission and fusion. STZ on ICV exposure cause a significant shift towards fission by upregulating protein expression and mitochondrial localization of Drp-1 (**p ≤ 0.01; Fig. 11c) and undermining the protein expression of Mfn2 (*p ≤ 0.05; Fig. 11b). FA supplementation has significantly mitigated the exacerbation in mitochondrial fission by downregulating expression and localization of Drp-1 on mitochondria (##p ≤ 0.01), FA also restored the Mfn2 protein expression (#p ≤ 0.05), and in-turn restored the mitophagy, a process responsible for removal of damaged mitochondria.

3.11. FA protects ICV –STZ induced mitochondrial dysfunction by upregulating PGC1-alpha

FA treatment has been found to have significantly (#p ≤ 0.05; Fig. 12) restored the ICV-STZ induced depletion in nuclear localization and protein expression of PGC-1 alpha. FA has been classically reported to increase PGC1-alpha expression, and the effect has been observed in ICV-STZ model of AD.

3.12. FA mitigates ICV-STZ induced mitochondrial Lipid peroxidation (LPO)

Mitochondrial membrane LPO has been considered as an important hallmark in the assessment of the extent of mitochondrial damage. FA treatment has been found to have a mitigatory role in (#p ≤ 0.05; Fig. 13) in ICV-STZ induced oxidative stress concomitant mitochondrial membrane damage (*p ≤ 0.05).

3.13. Effect of FA and ICV-STZ on ATP synthesis potential of mitochondria

FA treatment has been found to have a protective effect on F_1 –F_O synthase activity (#p ≤ 0.05; Fig. 14). F_1 –F_O synthase activity is the mainstay process in the mitochondria responsible for ATP synthesis potential of mitochondria, which is significantly impaired in ICV-STZ treated rat brain hippocampi (**p ≤ 0.01).

4. Discussion

There are extensive pieces of evidence available for the beneficial role of ferulic acid in various rodent models of toxicities at doses ranging from 50 mg/kg to 250 mg/kg (Kawabata et al., 2000). Humans may consume as much as 80–165 mg FA/meal, which corresponds to approximately 1–2 mg/kg of body weight (Barone et al., 2009). So, the current study was undertaken to evaluate the neuroprotective efficacy of FA on the administration of higher doses in ICV-STZ induced sporadic dementia and related mitochondrial abnormalities. ICV-STZ model has been proposed as a well characterized and is considered an appropriate non-transgenic model for sporadic dementia of Alzheimer's type (Grieb, 2016; Chen et al., 2013). ICV-STZ model of AD has been found to produce many pathological and molecular changes observed in human samples such as the presence of amyloid beta fibrils,

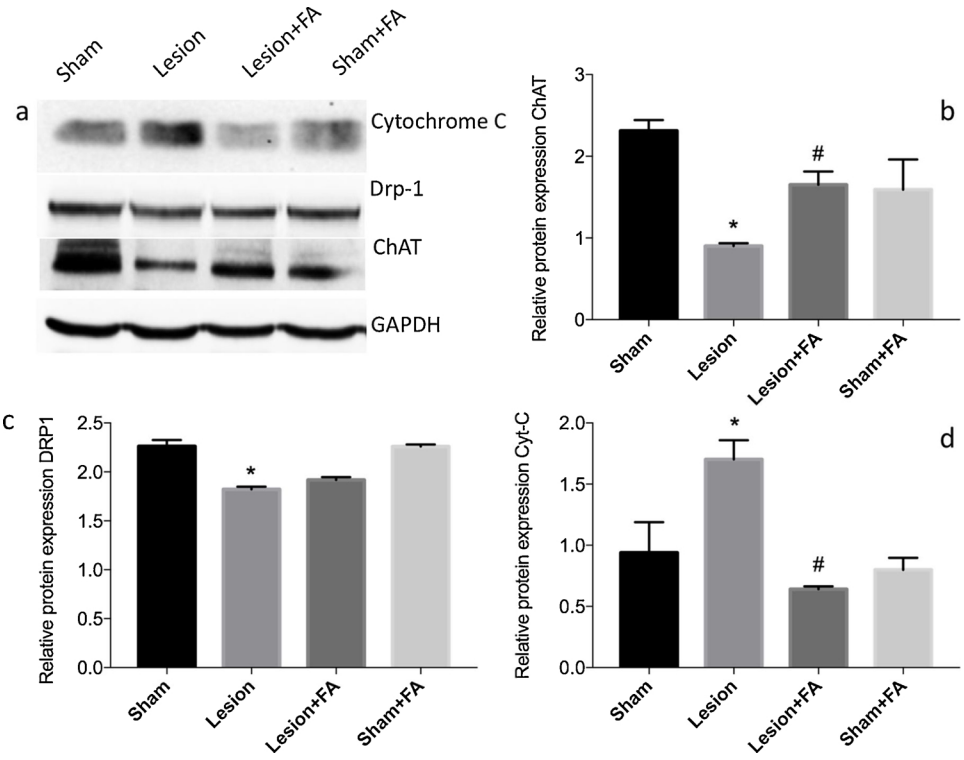

Fig. 9. Protein expression of GAPDH, ChAT, Drp-1, Bcl2 and Cytochrome-C an in FA and ICV-STZ treated rat brain hippocampi as compared with Sham. An equal amount of protein (35 µg) was separated on 10% TGX gels, immunoblotted and images were acquired using Bio-Rad ChemiDoc. Bands in Lane 1–4 shows expression profile in Sham, Lesion, Lesion + FA, and Sham + FA conditioned rats respectively. Values are expressed as Mean ± SEM as calculated using ImageJ (v1.50, NIH, USA). Significant differences were expressed as (*p ≤ 0.05) when the comparison was made with the Sham group and (#p ≤ 0.05) when compared with Lesion group.

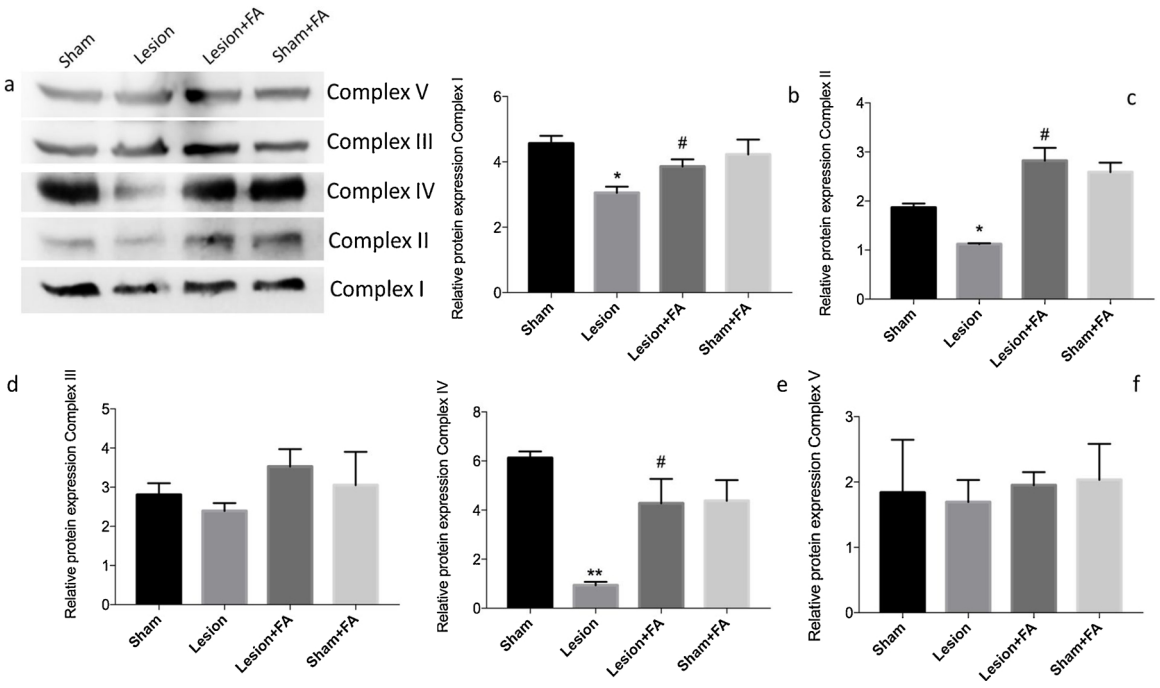

Fig. 10. Protein expression of OXPHOS in mitochondrial fraction of FA and ICV-STZ treated rat brain hippocampi as compared with Sham. An equal amount of protein (35 µg) was separated on 10% TGX gels, immunoblotted and images were acquired using Bio-Rad Chemi-Doc. Bands in Lane 1–4 shows expression profile in Sham, Lesion, Lesion + FA, and Sham + FA conditioned rats respectively. Values are expressed as Mean ± SEM as calculated using ImageJ (v1.50, NIH, USA). Significant differences were expressed as (*p ≤ 0.05) when the comparison was made with the Sham group and (#p ≤ 0.05) when compared with Lesion group.

hyperphosphorylation of tau, oxidative stress, cholinergic loss, neuroinflammation and mitochondrial abnormalities (Halawany, 2017; Ravelli et al., 2017; Kamat, 2015). Preservation of cholinergic function is vital for learning and memory, and its disruption is universal in cognitive impairments (Hasselmo, 2006). We have used morris water maze for assessment of the mitigatory role of FA on ICV-STZ related spatial learning and memory impairment. Our results have suggested that FA treatment has been able to decrease the escape latency (i.e., the time elapsed in finding the hidden platform), and increased the time spent by rats in the target quadrant during probe trial, suggesting better retention and recall of memory. The memory performance has been associated with the hippocampal morphology, and ICV-STZ has been reported to cause loss of pyramidal neuron in the CA1 region along with depletion of protein expression of ChAT (More et al., 2016; Wang et al., 2016; Dhull et al., 2012; Kraska et al., 2012). FA treatment has been found to restore the normal cellular morphology such as cell area and shape of pyramidal neurons in the CA1 region. FA treatment has also revived the protein expression of ChAT in the hippocampi of ICV-STZ

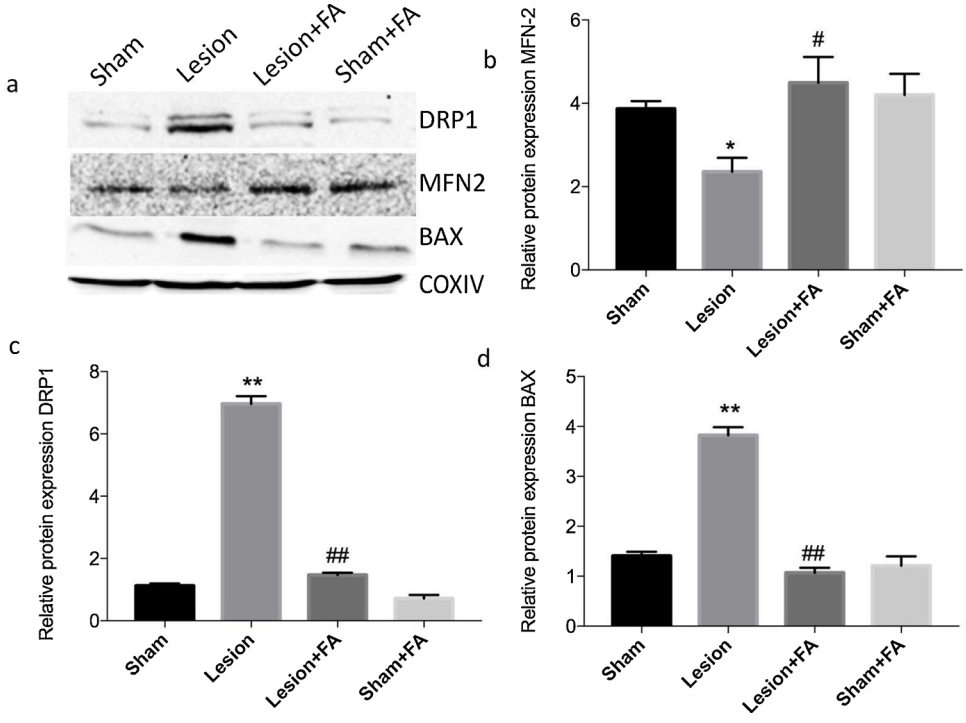

Fig. 11. Protein expression of Drp-1, Mfn2, and BAX in mitochondrial fraction of FA and ICV-STZ treated rat brain hippocampi as compared with Sham. An equal amount of protein (35 µg) was separated on 10% TGX gels, immunoblotted and images were acquired using BioRad Chemi-Doc. Bands in Lane 1–4 shows expression profile in Sham, Lesion, Lesion + FA, and Sham + FA conditioned rats respectively. Values are expressed as Mean ± SEM as calculated using ImageJ (version 1.50, NIH, USA). Significant differences were expressed as (*p ≤ 0.05) when the comparison was made with the Sham group and (#p ≤ 0.05) when compared with Lesion group.

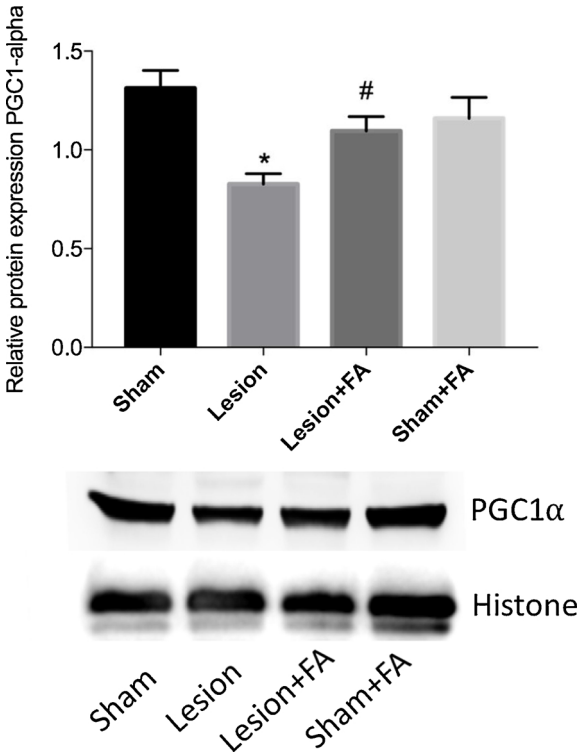

Fig. 12. Protein expression of PGC1-alpha in the nuclear fraction of FA and ICV-STZ treated rat brain hippocampi as compared with Sham. An equal amount of protein (35 µg) was separated on 10% TGX gels, immunoblotted and images were acquired using BioRad Chemi-Doc. Bands in Lane 1–4 shows expression profile in Sham, Lesion, Lesion + FA, and Sham + FA conditioned rats respectively. Values are expressed as Mean ± SEM as calculated using ImageJ (v1.50, NIH, USA). Significant differences were expressed as (*p ≤ 0.05) when the comparison was made with the Sham group and (#p ≤ 0.05) when compared with Lesion group.

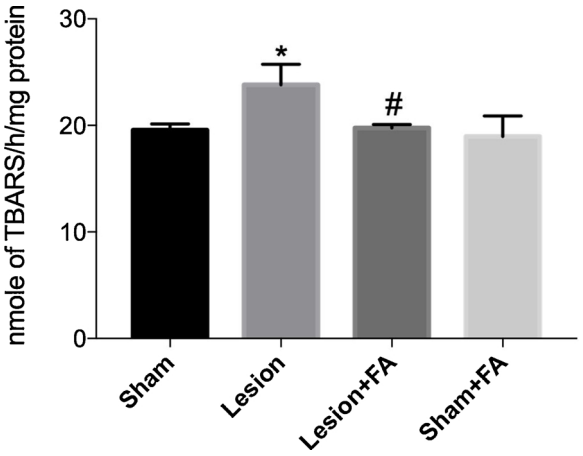

Fig. 13. Analysis of LPO levels in isolated mitochondria from hippocampi of rats from Sham, Lesion, Lesion + FA, and Sham + FA groups respectively. The results are expressed as nmoles of TBARS formed/ h/mg and were calculated using a molar extinction coefficient (MEC) $1.56 \times 105\ M^{-1}\,cm^{-1}$. Significant differences were expressed as (*p ≤ 0.05) when the comparison was made with the Sham group and (#p ≤ 0.05) when compared with Lesion group.

treated rats (Mancuso and Santangelo, 2014).

As numerous studies have reported exacerbation of ROS generation and concomitant apoptosis in AD (Guo et al., 2017a,b; Dhull et al., 2012; Reddy and Beal, 2008a), we analyzed the levels of Intracellular ROS by DCFDA. We also conducted GFAP and caspase3 activity

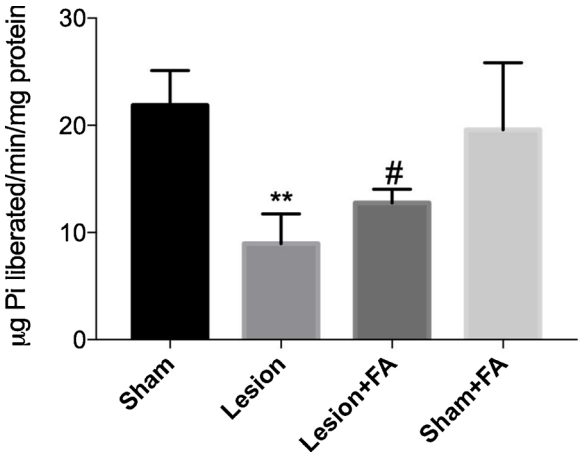

Fig. 14. $F_1 - F_O$ synthase activity for analysis of ATP synthesizing potential of mitochondrial isolated from Sham, Lesion, Lesion + FA, and Sham + FA groups respectively. Values are expressed as µmoles of Pi liberated/min/mg protein. Significant differences were expressed as (*p ≤ 0.05) when the comparison was made with the Sham group and (#p ≤ 0.05) when compared with Lesion group.

analysis, as astrogliosis and caspase3 activation is generally considered as the primary hallmark in hippocampal apoptosis (Günther et al., 2017; Rai et al., 2014).The results of our study showed that ICV-STZ administration at a subdiabetogenic dose of 3 mg/kg causes a significant increase in the intracellular ROS production, GFAP expression, caspase3 activation, and DNA fragmentation. These findings were well in accord with previous reports (Mishra et al.,2018; Nazifi et al.,2018). On the contrary, long-term oral gavage with FA has significantly mitigated the exacerbation of the ROS generation along with a decrease in GFAP expression, caspase 3 activation, and DNA fragmentation which generally collates with the studies advocating its antioxidant, anti-apoptotic and anti-inflammatory potential (He et al., 2018; Jain et al., 2018; Zhou et al., 2018).

Reactive oxygen species (ROS) are a frequent by-product of electron leakage from the inner mitochondrial membrane during mitochondrial oxidative phosphorylation. Under normal conditions, ROS are rapidly cleared to increasingly lesser reactive species by enzymes, but when mitochondria are perturbed, ROS production may exceed the cell's ability to neutralize, resulting in oxidative damage to the cell (Yu et al., 2018; Turrens, 2003). So, to further explore the effect of ICV-STZ model we have investigated the mitochondrial perturbations associated with it. Numerous studies have shown that hippocampal mitochondrial abnormalities are an integral part of transgenic and non-transgenic models of AD and have also been confirmed in the post-mortem samples (Cai and Tammineni, 2017; Guo et al., 2017a,b; Martins et al., 2016; Fernández-Moriano, 2015; Reddy et al., 2012; Reddy and Beal, 2008b). Recently, Paidi et al. (2015) have shown that ICV-STZ also presented the changes in mitochondrial dynamics as found in the human, affirming its suitability as a model of AD. Indeed, we have seen that the ICV administration of a sub-diabetogenic dose of STZ promotes a significant decline in hippocampal bioenergetics function as reflected by the decrease in the protein expression of OXPHOS complexes I, II and IV (Martins et al., 2016; Reddy and Beal, 2008a,b). This, in turn, leads to a decline in ($\Delta\psi m$) and increases the susceptibility for mPTP opening and further enhancing the oxidative damage, mitochondrial membrane damage (LPO), loss of ATP synthesizing capacity and progression of apoptosis by internalization of BAX into the mitochondria and release of Cytochrome C into the cytosol (Kim et al., 2018; Correia et al., 2013). FA treatment has been found to have a restorative effect on OXPHOS complexes, ATP synthesis and ($\Delta\psi m$), that may have caused the depletion of mPTP activity by limiting mitochondrial membrane damage, mitochondrial BAX expression and release of Cytochrome C responsible for caspase3 activation.

Moreover, we have found an increase and decrease in mitochondrial Drp1 and Mfn2 proteins levels respectively. Drp-1 being the critical effector of fission and its overexpression has been considered as a viable target for a therapeutic approach for AD (Kandimalla and Reddy, 2016; Manczak and Reddy, 2012). Additionally, Mfn2 has been a well-accredited marker and effector of mitochondrial fusion, depletion of Mfn2 causes depletion of mitochondrial trafficking and mitophagy. A balance between both the processes is essential for maintaining mitochondrial health of neurons (Reddy et al., 2011). ICV STZ enhances the localization of Drp-1 onto the outer mitochondrial membrane; this, in turn, decreases Mfn2 related fusion, causes ($\Delta\psi m$) loss and apoptosis (Tang et al., 2018). Interestingly, FA administration was able to restore the balance between these two processes.

Furthermore, Naik et al. (2017) has reported that ICV-STZ decreases mRNA expression of PGC1-alpha and rice bran oil has been reported to affect PGC1-alpha in aged NMRI mice (Hagl et al., 2016). PGC-1alpha has been accredited as the master regulator of mitochondrial biogenesis and currently no literature is available on its modulation by FA in ICV-STZ model. So, we have analyzed the effect of FA and ICV-STZ on PGC1-alpha nuclear protein levels and found that FA does increase the nuclear expression of PGC1-alpha levels as it is a transcription factor and its nuclear presence is of importance for mitochondrial biogenesis. In support of our finding, we have found that Peng et al. (2017); Singh et al. (2016); Lagouge et al. (2006) have shown that an increase in PGC1-alpha levels can modulate the promoter regions of Drp-1 and Mfn2 and can shift the balance to fusion by decrease Drp-1 expression and increasing Mfn2 expression. Our finding supports the protective efficacy of FA in AD-related neurodegeneration and concludes that FA may have the propensity to mitigate the apoptotic cell loss by the management of mitochondrial abnormalities associated with neurodegenerative damage.

References

Ansari, M.A., Scheff, S.W., 2010. Oxidative stress in the progression of alzheimer disease in the frontal cortex. J. Neuropathol. Exp. Neurol. 69 (2), 155–167.

Barone, E., Calabrese, V., Mancuso, C., 2009. Ferulic acid and its therapeutic potential as a hormetin for age-related diseases. Biogerontology 10 (2), 97–108.

Bradford, M.M., 1976. A rapid and sensitive method for the quantitation of microgram quantities of protein utilizing the principle of protein-dye binding. Anal. Biochem. 72, 248–254.

Cai, Q., Tammineni, P., 2017. Mitochondrial aspects of synaptic dysfunction in alzheimer's disease. J. Alzheimer Dis. 57 (4), 1087–1103.

Chen, Y., Liang, Z., Blanchard, J., et al., 2013. A non-transgenic mouse model (icv-STZ mouse) of Alzheimer's disease: Similarities to and differences from the transgenic model (3xTg-AD mouse). Mol. Neurobiol. 47 (2), 711–725.

Cheng, A., Hou, Y., Mattson, M.P., 2010. Mitochondria and neuroplasticity. ASN Neuro 2 (5), e00045.

Choi, J., Twamley, E.W., 2013. Cognitive rehabilitation therapies for Alzheimer's disease: a review of methods to improve treatment engagement and self-efficacy. Neuropsychol. Rev. 23 (1), 48–62.

Cornutiu, G., 2015. The Epidemiological Scale of Alzheimer's Disease. J. Clin. Med. Res. 7 (9), 657–666.

Correia, S.C., Santos, R.X., Santos, M.S., Casadesus, G., Lamanna, J.C., Perry, G., Smith, M.A., Moreira, P.I., 2013. Mitochondrial abnormalities in a streptozotocin-induced rat model of sporadic Alzheimer's disease. Curr. Alzheimer Res. 10 (4), 406–419.

Dhull, D.K., Jindal, A., Dhull, R.K., Aggarwal, S., Bhateja, D., Padi, S.S., 2012. Neuroprotective effect of cyclooxygenase inhibitors in ICV-STZ induced sporadic Alzheimer's disease in rats. J. Mol. Neurosci. 46 (1), 223–235.

Fernández-Moriano, C., González-Burgos, E., Gómez-Serranillos, M.P., 2015. Mitochondria-targeted protective compounds in parkinson's and alzheimer's diseases. Oxid. Med. Cell. Longev., 408927.

Ganguly, G., Chakrabarti, S., Chatterjee, U., Saso, L., 2017. Proteinopathy, oxidative stress, and mitochondrial dysfunction: cross talk in Alzheimer's disease and Parkinson's disease. Drug Des. Devel. Ther. 11, 797–810.

Gao, J., Wang, L., Liu, J., Xie, F., Su, B., Wang, X., 2017. Abnormalities of mitochondrial dynamics in neurodegenerative diseases. Yoon Y, ed.. Antioxidants 6 (2), 25.

Gella, A., Durany, N., 2009. Oxidative stress in Alzheimer disease. Cell Adh. Migr. 3 (1), 88–93.

Gomez-Nicola, D., Boche, D., 2015. Post-mortem analysis of neuroinflammatory changes in human Alzheimer's disease. Alzheimers Res. Ther. 7 (1), 42.

Grieb, P., 2016. Intracerebroventricular Streptozotocin Injections as a Model of Alzheimer's Disease: in Search of a Relevant Mechanism. Mol. Neurobiol. 53 (3), 1741–1752.

Günther, A., Luczak, V., Abel, T., Baumann, A., 2017. Caspase-3 and GFAP as early markers for apoptosis and astrogliosis in shRNA-induced hippocampal cytotoxicity. J. Exp. Biol. 220 (8), 1400–1404.

Guo, X.D., Sun, G.L., Zhou, T.T., Wang, Y.Y., Xu, X., Shi, X.F., Zhu, Z.Y., Rukachaisirikul, V., Hu, L.H., Shen, X., 2017a. LX2343 alleviates cognitive impairments in AD model rats by inhibiting oxidative stress-induced neuronal apoptosis and tauopathy. ActaPharmacol Sin. 38 (8), 1104–1119.

Guo, L., Tian, J., Du, H., 2017b. Mitochondrial Dysfunction and Synaptic Transmission Failure in Alzheimer's Disease. J. Alzheimer Dis. 57 (4), 1071–1086.

Gutiérrez-Rexach, J., Schatz, S., 2016. Cognitive impairment and pragmatics. SpringerPlus. 5, 127.

Hagl, S., Berressem, D., Grewal, R., Sus, N., Frank, J., Eckert, G.P., 2016. Rice bran extract improves mitochondrial dysfunction in brains of aged NMRI mice. Nutr. Neurosci. 19 (1), 1–10.

Halawany, Ali M.El, Sayed, NesrineS.E.L., Abdallah, HossamM., 2017. Riham Salah El Dine Protective effects of gingerol on streptozotocin-induced sporadic Alzheimer's disease: emphasis on inhibition of β-amyloid, COX-2, alpha-, beta - secretases and APH1a. Sci. Rep. 7, 2902.

Hasselmo, M.E., 2006. The role of acetylcholine in learning and memory. Curr. Opin. Neurobiol. 16 (6), 710–715.

He, S., Guo, Y., Zhao, J., Xu, X., Song, J., Wang, N., Liu, Q., 2018. Ferulic acid protects against heat stress-induced intestinal epithelial barrier dysfunction in IEC-6 cells via the PI3K/Akt-mediated Nrf2/HO-1 signaling pathway. Int. J. Hyperthermia 16, 1–10.

Jahn, H., 2013. Memory loss in Alzheimer's disease. Dialogues Clin. Neurosci. 15 (4), 445–454.

Jain, P.G., Mahajan, U.B., Shinde, S.D., Surana, S.J., 2018. Cardioprotective role of FA against isoproterenol induced cardiac toxicity. Mol. Biol. Rep Epub ahead of print.

Kamat, P.K., 2015. Streptozotocin induced Alzheimer's disease like changes and the underlying neural degeneration and regeneration mechanism. Neural Regen. Res. 10 (7), 1050–1052.

Kandimalla, R., Reddy, P.H., 2016. Multiple faces of dynamin-related protein 1 and its role in Alzheimer's disease pathogenesis. Biochim. Biophys. Acta 1862 (4), 814–828.

Kawabata, K., Yamamoto, T., Hara, A., Shimizu, M., Yamada, Y., Matsunaga, K., Tanaka, T., Mori, H., 2000. Modifying effects of ferulic acid on azoxymethaneinduced colon carcinogenesis in F344 rats. Cancer Lett. 157, 15–21.

Kelley, B.J., Petersen, R.C., 2007. Alzheimer's Disease and Mild Cognitive Impairment. Neurol. Clin. 25 (3), 577-v.

Kim, Y., Zheng, X., Ansari, Z., Bunnell, M.C., Herdy, J.R., Traxler, L., Lee, H., Paquola, A.C.M., Blithikioti, C., Ku, M., Schlachetzki, J.C.M., Winkler, J., Edenhofer, F., Glass, C.K., Paucar, A.A., Jaeger, B.N., Pham, S., Boyer, L., Campbell, B.C., Hunter, T., Mertens, J., 2018. Gage FH.Mitochondrial Aging Defects Emerge in Directly Reprogrammed Human Neurons due to Their Metabolic Profile. Cell Rep. 23 (9), 2550–2558.

Kraska, A., Santin, M.D., Dorieux, O., Joseph-Mathurin, N., Bourrin, E., Petit, F., Jan, C., Chaigneau, M., Hantraye, P., Lestage, P., Dhenain, M., 2012. In vivo cross-sectional characterization of cerebral alterations induced by intracerebroventricular administration of streptozotocin. PLoS One 7 (9), e46196.

Kumar, N., Pruthi, V., 2014. Potential applications of ferulic acid from natural sources. Biotechnol. Rep. 4, 86–93.

Lagouge, M., Argmann, C., Gerhart-Hines, Z., Meziane, H., Lerin, C., Daussin, F., Messadeq, N., Milne, J., Lambert, P., Elliott, P., Geny, B., Laakso, M., Puigserver, P., Auwerx, J., 2006. Resveratrol improves mitochondrial function and protects against metabolic disease by activating SIRT1 and PGC-1alpha. Cell. 127 (6), 1109–1122.

Lin, Y.H., Zhang, J.J., Chen, W.W., 1994. Protective effect of sodium ferulate on damage of the rat liver mitochondria induced by oxygen free radicals. Yao Xue Xue Bao 29 (3), 171–175.

Mancuso, C., Santangelo, R., 2014. Ferulic acid: pharmacological and toxicological aspects. Food Chem. Toxicol. 65, 185–195.

Manczak, M., Reddy, P.H., 2012. Abnormal interaction between the mitochondrial fission protein Drp1 and hyperphosphorylated tau in Alzheimer's disease neurons: implications for mitochondrial dysfunction and neuronal damage. Hum. Mol. Genet. 21 (11), 2538–2547.

Manczak, M., Calkins, M.J., Reddy, P.H., 2011. Impaired mitochondrial dynamics and abnormal interaction of amyloid beta with mitochondrial protein Drp1 in neurons from patients with Alzheimer's disease: implications for neuronal damage. Hum. Mol. Genet. 20 (13), 2495–2509.

Martins, I.V.A., Rivers-Auty, J., Allan, S.M., Lawrence, C.B., 2016. Mitochondrial abnormalities and synaptic loss underlie memory deficits seen in mouse models of obesity and alzheimer's disease. Moreira P, ed.. J. Alzheimer Dis. 55 (3), 915–932.

Mathew, S., Abraham, T.E., 2004. Ferulic acid: an antioxidant found naturally in plant cell walls and feruloyl esterases involved in its release and their applications. Crit. Rev. Biotechnol. 24 (2-3), 59–83.

Mishra, P., Chan, D.C., 2016. Metabolic regulation of mitochondrial dynamics. J. Cell Biol. 212 (4), 379–387.

Mishra, S.K., Singh, S., Shukla, S., Shukla, R., 2018. Intracerebroventricular streptozotocin impairs adult neurogenesis and cognitive functions via regulating neuroinflammation and insulin signaling in adult rats. Neurochem. Int. 113, 56–68.

More, S.V., Kumar, H., Cho, D.-Y., Yun, Y.-S., Choi, D.-K., 2016. Toxin-induced experimental models of learning and memory impairment. Lein P., ed.. Int. J. Mol. Sci. 17 (9), 1447.

Naik, B., Nirwane, A., Majumdar, A., 2017. Pterostilbene ameliorates intracerebroventricular streptozotocin induced memory decline in rats. Cogn. Neurodyn. 11 (1), 35–49.

Nazifi, M., Oryan, S., Eslimi Esfahani, D., Moghadamnia, A.A., Ashrafpour, M., 2018. Chronic Administration of Piperine Attenuates Behavioural, Biochemical and Histological Alterations induced by Intracerebroventricular Streptozotocin in Rats. Basic Clin. Pharmacol. Toxicol Epub ahead of print.

Paidi, R.K., Nthenge-Ngumbau, D.N., Singh, R., Kankanala, T., Mehta, H., Mohanakumar, K.P., 2015. Mitochondrial Deficits Accompany Cognitive Decline Following Single Bilateral Intracerebroventricular Streptozotocin. Curr. Alzheimer Res. 12 (8), 785–795.
Paxinos, G., Watson, C., 1986. The Rat Brain in Stereotaxic Coordinate. Academic Press, Sydney.
Peng, K., Yang, L., Wang, J., Ye, F., Dan, G., Zhao, Y., Cai, Y., Cui, Z., Ao, L., Liu, J., Zou, Z., Sai, Y., Cao, J., 2017. The interaction of mitochondrial biogenesis and Fission/Fusion mediated by PGC-1α regulates rotenone-induced dopaminergic neurotoxicity. Mol. Neurobiol. 54 (5), 3783–3797.
Picone, P., Nuzzo, D., Di Carlo, M., 2013. Ferulic acid: a natural antioxidant against oxidative stress induced by oligomeric A-beta on sea urchin embryo. Biol. Bull. 224 (1), 18–28.
Rai, S., Kamat, P.K., Nath, C., Shukla, R., 2014. Glial activation and post-synaptic neurotoxicity: the key events in Streptozotocin (ICV) induced memory impairment in rats. Pharmacol. Biochem. Behav. 117, 104–117.
Ravelli, K.G., Rosário, B.D., Camarini, R., Hernandes, M.S., Britto, L.R., 2017. Intracerebroventricular streptozotocin as a model of alzheimer's disease: neurochemical and behavioral characterization in mice. Neurotox. Res. 31 (3), 327–333.
Reddy, P.H., Beal, M.F., 2008a. Amyloid beta, mitochondrial dysfunction and synaptic damage: implications for cognitive decline in aging and Alzheimer's disease. Trends Mol. Med. 14 (2), 45–53.
Reddy, P.H., Beal, M.F., 2008b. Amyloid beta, mitochondrial dysfunction and synaptic damage: implications for cognitive decline in aging and Alzheimer's disease. Trends Mol. Med. 14 (2), 45–53.
Reddy, P.H., Reddy, T.P., Manczak, M., Calkins, M.J., Shirendeb, U., Mao, P., 2011. Dynamin-related protein 1 and mitochondrial fragmentation in neurodegenerative diseases. Brain Res. Rev. 67 (1-2), 103–118.
Reddy, P.H., Tripathy, R., Troung, Q., et al., 2012. Abnormal mitochondrial dynamics and synaptic degeneration as early events in alzheimer's disease: implications to mitochondria-targeted antioxidant therapeutics. Biochim. Biophys. Acta 1822 (5), 639–649.
Robert, P., Ferris, S., Gauthier, S., Ihl, R., Winblad, B., Tennigkeit, F., 2010. Review of Alzheimer's disease scales: is there a need for a new multi-domain scale for therapy evaluation in medical practice? Alzheimers Res. Ther. 2 (4), 24.
Russ, T.C., Gatz, M., Pedersen, N.L., et al., 2015. Geographical variation in dementia: examining the role of environmental factors in Sweden and Scotland. Epidemiology 26 (2), 263–270.
Safiulina, D., Kaasik, A., 2013. Energetic and dynamic: how mitochondria meet neuronal energy demands. PLoS Biol. 11 (12), e1001755.
Selkoe, D.J., Lansbury Jr., P.J., et al., 1999. Alzheimer's disease Is the Most Common neurodegenerative disorder. In: Siegel, G.J., Agranoff, B.W., Albers, R.W. (Eds.), Basic Neurochemistry: Molecular, Cellular and Medical Aspects, 6th ed. Lippincott-Raven, Philadelphia.
Singh, S.P., Schragenheim, J., Cao, J., Abraham, N.G., Bellner, L., 2016. PGC-1 alpha Regulates HO-1 Expression, Mitochondrial Dynamics and Biogenesis: Role of Epoxyeicosatrienoic Acid. Prostaglandins Other Lipid Mediat. 125, 8–18.
Swerdlow, R.H., 2012. Mitochondria and cell bioenergetics: increasingly recognized components and a possible etiologic cause of alzheimer's disease. Antioxid. Redox Signal. 16 (12), 1434–1455.
Tang, Q., Liu, W., Zhang, Q., Huang, J., Hu, C., Liu, Y., Wang, Q., Zhou, M., Lai, W., Sheng, F., Li, G., Zhang, R., 2018. Dynamin-related protein 1-mediated mitochondrial fission contributes to IR-783-induced apoptosis in human breast cancer cells. J. Cell. Mol. Med Epub ahead of print.
Turrens, J.F., 2003. Mitochondrial formation of reactive oxygen species. J. Physiol. (Lond.) 552 (2), 335–344.
United Nations, 2015. Department of Economic and Social Affairs, Population Division. World Population Ageing ST/ESA/SER.A/390.
Wallace, D.C., 2013. A mitochondrial bioenergetic etiology of disease. J. Clin. Invest. 123 (4), 1405–1412.
Wang, X., Su, B., Lee, H.G., Li, X., Perry, G., Smith, M.A., Zhu, X., 2009. Impaired balance of mitochondrial fission and fusion in Alzheimer's disease. J. Neurosci. 29 (28), 9090–9103.
Wang, H., Wang, H., Cheng, H., Che, Z., 2016. Ameliorating effect of luteolin on memory impairment in an Alzheimer's disease model. Mol. Med. Rep. 13 (5), 4215–4220.
WHO, 2012. In: WHO (Ed.), Dementia: a Public Health Priority. WHO, Geneva.
Wu, Z.J., Yu, J., Fang, Q.J., Lian, J.B., Wang, R.X., He, R.L., Lin, M.J., 2014. Sodium ferulate protects against daunorubicin-induced cardiotoxicity by inhibition of mitochondrial apoptosis in juvenile rats. J. Cardiovasc. Pharmacol. 63 (4), 360–368.
Yan, J.J., Cho, J.Y., Kim, H.S., Kim, K.L., Jung, J.S., Huh, S.O., Suh, H.W., Kim, Y.H., Song, D.K., 2001. Protection against beta-amyloid peptide toxicity in vivo with long-term administration of ferulic acid. Br. J. Pharmacol. 133 (1), 89–96.
Yu, H., Lin, X., Wang, D., et al., 2018. Mitochondrial molecular abnormalities revealed by proteomic analysis of hippocampal organelles of mice triple transgenic for alzheimer disease. Front. Mol. Neurosci. 11, 74.
Zhou, Q., Gong, X., Kuang, G., Jiang, R., Xie, T., Tie, H., Chen, X., Li, K., Wan, J., Wang, B., 2018. Ferulic acid protected from kidney ischemia-reperfusion injury in mice: possible mechanism through increasing adenosine generation via HIF-1α. Inflammation Epub ahead of print.
Zhu, X., Perry, G., Smith, M.A., Wang, X., 2013. Abnormal mitochondrial dynamics in the pathogenesis of Alzheimer's disease. J. Alzheimers Dis. 33 (Suppl. 1), S253–S262.
Zhu, H., Liang, Q.H., Xiong, X.G., Chen, J., Wu, D., Wang, Y., Yang, B., Zhang, Y., Zhang, Y., Huang, X., 2014. Anti-Inflammatory effects of the bioactive compound ferulic acid contained in oldenlandia diffusa on collagen-induced arthritis in rats. Evid. Complement. Alternat. Med. 2014, 573801.